Theor Chem Acc (2010) 127:759–763
DOI 10.1007/s00214-010-0804-9

REGULAR ARTICLE

Theoretical investigation into charge mobility in 4,4′-bis(1-naphthylphenylamino)biphenyl

Hongze Gao

Received: 14 July 2010 / Accepted: 22 August 2010 / Published online: 1 September 2010

Abstract Density functional theory (DFT) and Marcus charge transport theory were employed to investigate the charge transport properties of 4,4′-bis(1-naphthylphenylamino)biphenyl (NPB), which is widely used as hole-transport material in organic photoelectron devices. Using an incoherent transport model, we respectively calculated its electron and hole mobility (μ). It has high electron-transport efficiency ($\mu_{electron} = 1.43 \times 10^{-2}$ cm^2/(V·s)) than that of hole ($\mu_{hole} = 1.62 \times 10^{-3}$ cm^2/(V·s)). The results are consistent with the experiment Tse et al. (Appl Phys Lett 89, 262102, 2006), and the difference was explained in terms of the spatial extent of the frontier orbitals.

Keywords DFT · Charge transport · Marcus theory · 4,4′-bis(1-naphthylphenylamino)biphenyl (NPB)

1 Introduction

Poly(aryl)amines are now widely used as hole-transport materials in applications ranging from the xerox process to multilayer organic light-emitting diode (OLED)-based devices. Though N,N′-diphenyl-N,N′-bis(3-methylphenyl)-(1,1′-biphenyl)-4,4′-diamine (TPD) and NPB are most widely used as hole-transport materials, only several authors have used computational methods to address the structure–property issues in TPD-derived molecular materials, with particular emphasis on the geometric and electronic changes which accompany oxidation/hole-transport phenomena [1–8]. Although these pioneering studies have been important for understanding the transport of charge carriers in OLED materials on the molecular level, only the reorganization energies of these poly(aryl)amines are considered. Interestingly, for most compounds of poly(aryl)amines, the reorganization energy for the hole transport is larger than for the electron transport except NPB [1]. So, the following question comes out: Whether the electron mobility of NPB is really larger than its hole mobility? Tse et al. [9] have proved that the NPB has good electron transport capability. But the reason remains unclear. According to Marcus theory [10], the important parameters to characterize the carrier mobility are electronic coupling term and reorganization energy. So, if the question be answered, the electronic coupling of NPB must be considered. In context, density functional theory (DFT) method and Marcus theory were employed to investigate both electron and hole-transport properties of NPB.

2 Computational methods and theory

The hopping model theory [11] is suitable for our case, because the intermolecular interactions are weak for the most thin-film amorphous materials in OLEDs. Within the present simple model, even though the crystal structure is employed here in defining all the charge transport pathways, the results also can be relevant for the thin films. In fact, in this approach, the charge is assumed to be localized in one molecule, instead of spreading out in the bulk. A good thin film is usually quite ordered up to a few hundred nanometers in size [12, 13]. The effects of grain boundaries and charge traps were neglected for a pure crystal, if the intermolecular interaction is strong, the charge could not be assumed to be localized in the molecule; thus, the present

H. Gao (✉)
Fundamental Department,
Chinese People's Armed Police Force Academy,
Langfang 065000, Hebei, People's Republic of China
e-mail: gaohz06@mails.jlu.edu.cn

model could not be applied. However, for the NPB we studied, we note that V $\ll \lambda$. It is to say the intermolecular coupling is much less important than the charge relaxation. So, the Marcus theory is fully applicable, and the results presented in this work could shed light on materials design for organic semiconductors.

In these cases, the charge transport mechanism can be described as a self-exchange electron-transfer reaction from a charged oligomer to an adjacent neutral oligomer and vice versa. According to the semiclassical electron-transfer theory [10], the charge-transfer rate, k_{ET}, can be described as:

$$k_{ET} = \frac{4\pi^2}{h}\frac{1}{\sqrt{4\pi\lambda k_B T}}V^2 \exp\left(-\frac{\lambda}{4k_B T}\right) \quad (1)$$

where λ is the reorganization energy, V is the transfer integral, T is the temperature, and h and k_B are the Planck and Boltzmann constants, respectively. The intermolecular transfer integral V characterizes the strength of electronic coupling between the two oligomers. The charge-transfer integrals for charge transport are obtained from the direct method [12–15] and can be written as:

$$V = \left\langle \phi_{MO}^{0,\text{site1}} | F | \phi_{MO}^{0,\text{site2}} \right\rangle \quad (2)$$

where $\phi_{MO}^{0,\text{site1}}$ and $\phi_{MO}^{0,\text{site2}}$ represent the LUMOs for electron transport (HOMOs for hole transport) of isolated molecules 1 and 2, respectively, and F is the Fock operator for the dimer with a density matrix from noninteracting dimer of $F = SC\varepsilon C{-}1$, where S is the intermolecular overlap matrix, and C and ε are the molecular orbital coefficients and energies from one-step diagonalization without iteration. The charge-transfer integral calculations were performed using the PW91PW91/6-31G* method. It has been proven that this choice of functional gives the best results at the DFT level [15, 16].

The reorganization energy is the sum of two energetic terms: the inner reorganization energy of the molecule and the reorganization energy of surrounding medium. In this case, the latter contribution can be neglected, so that the structural differences between the equilibrium configurations of π-conjugated units in neutral and ionic states become the dominant ones [17]. The internal reorganization energies for electrons and holes transport calculated by the DFT B3LYP/6-31G* method. The reorganization energy (λ) corresponds to the sum of geometry relaxation energies upon going from the neutral-state geometry to the charged-state geometry and vice versa. Hence, λ for charge transfer is given by

$$\lambda = [E^{\text{ion}}(g^0) - E^{\text{ion}}(g^{\text{ion}})] + [E^0(g^{\text{ion}}) - E^0(g^0)] \quad (3)$$

Here, $E^{\text{ion}}(g^0)$ and $E^0(g^0)$ are the energy of the ionic and neutral state with the optimized geometry of the neutral molecule, respectively; $E^{\text{ion}}(g^{\text{ion}})$ and $E^0(g^{\text{ion}})$ are the energy of the ionic and neutral states with the optimized ionic geometry, respectively.

Given the hopping rate between two neighbors, for a spatially isotropic system, the homogeneous diffusion constant D can be approximately evaluated by [18]:

$$D = \frac{1}{2n}\sum_i r_i^2 k_i P_i \quad (4)$$

where $n = 3$ is the dimensionality, k_i is the hopping rate due to charge carrier to the ith neighbor, r_i is the distance to neighbor i, P_i is the relative probability for charge carrier to a particular ith neighbor:

$$P_i = k_i \Big/ \sum_i k_i \quad (5)$$

Summing over all possible hops leads to the diffusion coefficient in Eq. 4. The drift mobility of hopping, μ, is then evaluated from the Einstein relation,

$$\mu = \frac{e}{k_B T} D \quad (6)$$

Here, e is the electron charge.

The geometry (Fig. 1) optimizations were performed at the density functional theory level with the B3LYP functional using the Gaussian 03 program suite [19], involving the gradient correction of the exchange functional by Becke [20, 21] and the correction functional by Lee et al. [22], employing a 6-31G* split-valence basis set which has been proven reasonable for the system [1, 8, 23]. Subsequently, vibrational frequencies were performed at the same theoretical level to confirm that the ground-state conformation was a minimum on the potential energy surface. The cationic and anionic states were also optimized with an unrestricted B3LYP functional, and spin contamination in the radical species was found to be very small ($\langle S2 \rangle \leq 0.75$). C2 symmetry was adopted during optimization.

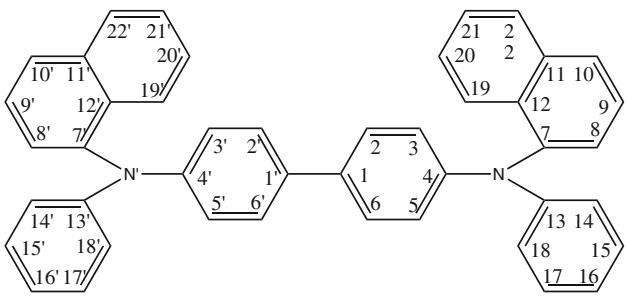

Fig. 1 Chemical structure of NPB and series number

3 Results and discussion

3.1 Geometry and reorganization energy

The initial ground-state geometry of NPB was obtained from the experimental results determined by the single-crystal X-ray diffraction [24] and fully optimized. Table 1 summarizes some key geometry parameters [25] optimized for the ground, cationic, and anionic states of the NPB. Note that △(C-G) represents the geometry difference between optimized cationic geometry and optimized neutral geometry, and △(A-G) denotes the geometry modifications between optimized anionic geometry and optimized neutral one. The optimized geometries agree well with other density functional calculations [1, 8, 23].

The reorganization energy in NPB for electron (λ_e) and hole (λ_h) computed are 0.158 and 0.295 eV, respectively. And the calculated charge carrier organization energies are in agreement with other DFT calculation [1, 23]. The larger reorganization energy of the hole is rationalized by the fact that the key geometry modifications except dihedral angle $D_{14\text{-}13\text{-}N\text{-}4}$ upon oxidation are bigger than upon reduction (see Table 1). According to Eq. 1, though NPB is a well-known hole-transport material, it may be a better electron transporter from the point of view of reorganization energy. So, the answer may be obtained from charge-transfer integrals.

3.2 Charge-transfer integrals and charge mobility

The relative positions of the two molecules in the hopping complexes are necessary for calculating transfer integral in an amorphous film. An amorphous material can be considered as a collection of molecules with relative positions similar to that in crystalline state without long-range order. Here, we use the single-crystal structure of NPB [24] to generate all the possible nearest-neighbor intermolecular hopping pathways (dimers). All the hopping pathways are shown in Fig. 2. Once a transport pathway is defined, the charge-transfer integral can be obtained by direct dimer Hamiltonian evaluation method [12–15]. Diffusion coefficient (D) and drift mobility (μ) for electron and hole in the NPB were estimated from Eqs. 4, 5, and 6 computed at 300K. The dimer center mass (CM) distance, transfer integral (V) are presented in Table 2.

Table 2 The dimer center mass (CM) distance and transfer integrals calculated of NPB

Path way	Dimer CM distance (Å)	Transfer integral/10^{-6} eV	
		Hole	Electron
1	10.090	165.02	2.43
2	11.338	1,504.20	619.47
3	9.575	3,320.21	5,217.35
4	9.950	4,228.61	1,520.86
5	11.338	1,504.20	619.47
6	12.359	428.37	8,67.07
7	10.309	121.47	91.56
8	10.252	3,319.16	5,263.15
9	12.359	428.37	867.07
10	10.309	121.47	91.56
11	9.950	4,228.61	1,520.86
12	10.144	165.39	2.80

Table 1 Selected calculated ground, cationic, and anionic bond lengths (Å), bond angle (°), and dihedral angle (°) for the NPB

	$R_{1\text{-}1'}$	$R_{4\text{-}N}$	$R_{7\text{-}N}$	$R_{13\text{-}N}$	$A_{4\text{-}N\text{-}7}$	$A_{4\text{-}N\text{-}13}$	$A_{7\text{-}N\text{-}13}$	$D_{6\text{-}1\text{-}1'\text{-}6'}$	$D_{7\text{-}N\text{-}13\text{-}4}$	$D_{8\text{-}7\text{-}N\text{-}4}$	$D_{14\text{-}13\text{-}N\text{-}4}$
Ground	1.482	1.421	1.431	1.419	118.2	121.2	119.5	35.3	167.9	54.9	−140.9
Cation	1.457	1.388	1.438	1.430	119.4	121.9	118.3	19.8	173.5	59.9	−136.1
△(C-G)	−0.025	−0.033	0.007	0.011	1.2	0.7	−1.2	−15.5	5.6	5.0	4.8
Anion	1.473	1.423	1.434	1.407	117.3	121.6	120.6	27.8	171.6	60.7	−153.3
△(A-G)	−0.009	0.002	0.003	−0.012	−0.9	0.4	1.1	−7.5	3.7	5.8	−12.4

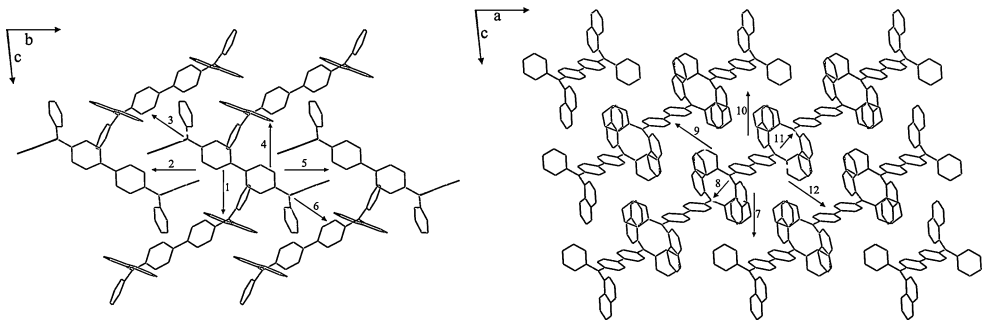

Fig. 2 Charge hopping pathways for NPB

Fig. 3 The frontier orbitals of **NPB**

Considering all the pathways, the largest transfer integrals are about 0.004 eV in the pathways 4, 11 for hole and 0.005 eV in the pathway 8 for electron, respectively. Different pathways have different contribution to the charge mobility. These indicate that the charge mobility is quite anisotropic. To understand the magnitude of the transfer integral values, we need to examine the packing of molecules in crystal structure. The magnitudes of V depend on the overlap degree between the HOMOs of the hopping complex for hole (LUMOs for electron). For example, when there is obvious HOMO orbitals overlap between two molecules in a dimer, the V values for hole will be large, which could be demonstrated in the case of the pathway 4 (see Fig. 2).

The electron drift mobility (μ, 1.43×10^{-2} $cm^2/(V{\cdot}s)$) is more than 1 orders of magnitude larger than the hole drift mobility (1.62×10^{-3} $cm^2/(V{\cdot}s)$). Both electron drift mobility and hole drift mobility are higher than the experimental results [9, 26], and this indicates that its charge mobilities could be improved through controlling the operation process in the OLED technology. Since electrons are sequentially transferred through the lowest unoccupied molecular orbital (LUMO) for electron transport and through the highest occupied molecular orbital (HOMO) for hole transport in organic disordered systems [27], the result can be rationalized from frontier orbitals of NPB (Fig. 3). The HOMO in NPB is mainly from the biphenyl and benzene rings connected with N atom, while its LUMO localizes at the naphthyl groups. And naphthyl group bulge on the outside of the molecule, so the LUMO component characteristic is conducive to orbital overlap among molecules and improve the electron transport efficiency.

4 Conclusion

On the bases of optimized equilibrium geometries of neutral, cationic, and anionic states of **NPB** by means of the B3LYP, the inner reorganization energies (λ) for hole and electron were obtained. The transfer integrals were calculated using direct dimer Hamiltonian evaluation method. The electron drift mobility (μ, 1.43×10^{-2} $cm^2/(V{\cdot}s)$) is more than 1 orders of magnitude larger than the hole drift mobility (1.62×10^{-3} $cm^2/(V{\cdot}s)$). So, **NPB** is not only a hole-transporting material but also a better electron-transporting material. The result is in agreement with the experimental reports.

Acknowledgments The author thanks the Institute of Functional Material Chemistry, Faculty of Chemistry (Northeast Normal University, People's Republic of China) for computational support and Open Project Program of State Key Laboratory of Supramolecular Structure and Materials, Jilin University.

References

1. Lin BC, Cheng CP, Lao ZPM (2003) J Phys Chem A 107:5241–5251
2. Malagoli M, Manoharan M, Kippelen B, Bredas JL (2002) Chem Phys Lett 354:283–290
3. Malagoli M, Bredas JL (2000) Chem Phys Lett 327:13–17
4. Sakanoue K, Motoda M, Sugimoto M, Sakaki S (2000) Nonlinear Optic Princ Mater Phenom Dev 26:271–278
5. Sakanoue K, Motoda M, Sugimoto M, Sakaki S (1999) J Phys Chem A 103:5551–5556
6. Aratani S, Kawanishi T, Kakuta A (1996) Jpn J Appl Phys Part 1 35:2184–2189
7. Aratani S, Kawanishi T, Kakuta A (1991) Jpn J Appl Phys 30:L1656–L1658
8. Wang BC, Liao HR, Chang JC, Chen L, Yeh JT (2007) J Lumin 124:333–342
9. Tse SC, Kwok KC, So SK (2006) Appl Phys Lett 89:262102
10. Marcus RA (1993) Rev Mod Phys 65:599–610
11. Marcus RA, Sutin N (1985) Biochim Biophys Acta 811:265–322
12. Yang XD, Wang LJ, Wang CL, Long W, Shuai ZG (2008) Chem Mater 20:3205–3211
13. Wang LJ, Nan GJ, Yang XD, Peng Q, Li QK, Shuai ZG (2010) Chem Soc Rev 39:423–434
14. Yang XD, Li QK, Shuai ZG (2007) Nanotechnology 18:424029
15. Troisi A, Orlandi G (2001) Chem Phys Lett 344:509–518
16. Song YB, Di CA, Yang XD, Li SP, Xu W, Liu YQ, Yang LM, Shuai ZG, Zhang DQ, Zhu DB (2006) J Am Chem Soc 128:15940–15941
17. Berlin YA, Hutchison GR, Rempala P, Ratner MA, Michl J (2003) J Phys Chem A 107:3970–3980
18. Deng WQ, Goddard WA (2004) J Phys Chem B 108:8614–8621
19. Frisch MJ, Trucks GW, Schlegel HB, Scuseria GE, Robb MA, Cheeseman JR, Montgomery JA Jr, Vreven T, Kudin KN, Burant JC, Millam JM, Iyengar SS, Tomasi J, Barone V, Mennucci B, Cossi M, Scalmani G, Rega N, Petersson GA, Nakatsuji H, Hada M, Ehara M, Toyota K, Fukuda R, Hasegawa J, Ishida M, Nakajima T, Honda Y, Kitao O, Nakai H, Klene M, Li X, Knox JE, Hratchian HP, Cross JB, Adamo C, Jaramillo J, Gomperts R, Stratmann RE, Yazyev O, Austin AJ, Cammi R, Pomelli C, Ochterski JW, Ayala PY, Morokuma K, Voth GA, Salvador P,

Dannenberg JJ, Zakrzewski VG, Dapprich S, Daniels AD, Strain MC, Farkas O, Malick DK, Rabuck AD, Raghavachari K, Foresman JB, Ortiz JV, Cui Q, Baboul AG, Clifford S, Cioslowski J, Stefanov BB, Liu G, Liashenko A, Piskorz P, Komaromi I, Martin RL, Fox DJ, Keith T, Al-Laham MA, Peng CY, Nanayakkara A, Challacombe M, Gill PMW, Johnson B, Chen W, Wong MW, Gonzalez C, Pople JA (2003) Gaussian 03, Revision C.02. Gaussian, Inc., Pittsburgh, PA
20. Becke AD (1988) Phys Rev A 38:3098–3100
21. Becke AD (1993) J Chem Phys 98:1372–1377
22. Lee CT, Yang WT, Parr RG (1988) Phys Rev B 37:785–789
23. Zou LY, Ren AM, Feng JK, Ran XQ (2009) J Phys Org Chem 22:1104–1113
24. Huang LQ, Cao QY, Yi C, Yang CJ, Gao XC (2006) Acta Crystallogr E 62:O2075–O2076
25. Low PJ, Paterson MAJ, Yufit DS, Howard JAK, Cherryman JC, Tackley DR, Brook R, Brown B (2005) J Mater Chem 15:2304–2315
26. Chen CH, Huang SW (2007) Organic electroluminescent materials & devices. Tsinghua University Press, Beijing
27. Shirota Y, Kageyama H (2007) Chem Rev 107:953–1010